Published in final edited form as:
Heart Rhythm. 2008 June ; 5(6): 787–793. doi:10.1016/j.hrthm.2008.03.003.

Cardiac Cycle Dependent Left Atrial Dynamics: Implications for Catheter Ablation of Atrial Fibrillation

Amit R. Patel, MD, **Omid Fatemi, MD**, **Patrick T. Norton, MD**, **J. Jason West, MD**, **Adam S. Helms, MD**, **Christopher M. Kramer, MD**, and **John D. Ferguson, MBChB MD**
University of Virginia, Charlottesville, VA Departments of Medicine (ARP, OF, JW, AH, CMK, JDF) and Radiology (PTN, CMK)

Abstract

Background—Left atrial volume (LAV) determines prognosis and response to therapy in atrial fibrillation. Integration of electro-anatomical maps with 3D-images rendered from CT and MRI is used to facilitate atrial fibrillation ablation.

Objectives—We measured LAV changes and regional motion during the cardiac cycle that might affect the accuracy of image integration and determined their relationship to standard LAV measurements.

Methods—MRI was performed in thirty patients with paroxysmal atrial fibrillation. Left atrial time-volume curves were generated and used to divide the left atrial function (LAEF) into pumping (PEF) and conduit (CEF) fractions and to determine the maximum LAV (LAMAX) and the pre-atrial contraction volume (PACV). LAV was measured using an MRI angiogram and traditional geometric models from echocardiography (area-length and ellipsoid). The in-plane displacement of the pulmonary veins, anterior left atrium, mitral annulus, and left atrial appendage was measured.

Results—LAMAX was 107±36ml and occurred at 42±5% of the RR interval. PACV was 86 ±34ml and occurred at 81±4% of the RR interval. LAEF was 45±10% and PEF was 31±10%. LAV measurements made from the MRI angiogram, area-length and ellipsoid models underestimated LAMAX by 21±25ml, 16±26ml, and 35±22ml, respectively. The anterior LA, mitral annulus, and left atrial appendage were significantly displaced during the cardiac cycle (8.8±2.0mm, 13.2±3.8mm, and 10.2±3.4mm, respectively); the pulmonary veins were not.

Conclusions—LAV changes significantly during the cardiac cycle and substantial regional variation in left atrial motion exists. Standard measurements of left atrial volume significantly underestimate LAMAX when compared to the gold standard measure of 3D-volumetrics.

Keywords

Atrial fibrillation; magnetic resonance imaging; MR imaging; atrial anatomy; atrial morphology; atrial mapping; atrial fibrillation ablation; left atrium

Correspondence to: John D. Ferguson, MBChB MD, University of Virginia Health System, Department of Medicine, 1215 Lee Street, Box 800158, Charlottesville, VA 22908, E-mail: jdf7h@virginia.edu, Telephone: (434) 982-3367, Fax: (434) 924-2581.

Disclosures: The authors do not have any conflicts of interest.

Background

Atrial fibrillation (AF) ablation is recommended and is increasingly being adopted as second line therapy in patients with symptomatic AF unresponsive to anti-arrhythmic drugs(1–3). Manipulation of an ablation catheter in the left atrium (LA) can be time consuming and involve significant fluoroscopy, but new technologies are evolving to facilitate catheter navigation and reduce procedure and fluoroscopy times(4–7). Recently, mapping systems have incorporated three-dimensional (3D) cardiac computed tomography (CCT) and cardiac magnetic resonance (CMR) imaging of the LA to facilitate nonfluoroscopic mapping(8–11). These data sets can be displayed side by side with a catheter geometry, providing an anatomical reference (Digital Image Fusion™, EnSite 5.01 workstation, Endocardial Solutions, Inc., MN), or as an image registered with the catheter geometry (Carto XP™, Biosense Webster, Diamond Bar, CA and EnSite Fusion™, Endocardial Solutions, Inc., MN).

CCT or CMR 3D images provide remarkable definition of the LA anatomy and are helpful in defining the number, location and size of the pulmonary veins, the relationship of the left upper pulmonary vein to the left atrial appendage and the LA relations to the esophagus, aorta and pulmonary artery. This 3D display provides a better understanding of the complex LA anatomy than the two dimensional views from fluoroscopy, pulmonary venograms or intra-cardiac echocardiography and offers the potential to improve catheter navigation and increase accuracy of ablation lesion placement(12,13).

Nevertheless, the 3D image is a static ‘snapshot’ in time during the cardiac cycle. Changes in the volume and shape during the cardiac cycle may significantly alter the dimensions of the static 3D image. We hypothesized that cycle dependent changes could alter the accuracy of 3D image registration with the catheter geometries. Thus, we used CMR to quantify the changes in LA volume (LAV) and regional displacement during the cardiac cycle.

Methods

We studied 30 consecutive patients in sinus rhythm with a history of paroxysmal atrial fibrillation referred for CMR prior to atrial fibrillation ablation. Patients were included in the study if they were ≥ 18 years and had a history of paroxysmal atrial fibrillation refractory to ≥ 2 anti-arrhythmic drugs. Patients with a history of congestive heart failure, valvular heart disease, or a left ventricular ejection fraction <45% were excluded.

CMR Imaging

The study was performed on a 1.5 Tesla Siemens Avanto MRI scanner (Siemens Medical Solutions, Erlangen, Germany). Using steady state free precession imaging (SSFP, TR 3ms, TE 1.1–1.3ms), retrospectively gated, 6mm thick axial cines with 25 to 40 frames per cardiac cycle spanning the entire left atrium were obtained without gap between slices. SSFP cines were also acquired in 2-chamber, 3-chamber and 4-chamber orientations. A breath-held, non-gated MRA in the coronal plane was performed using 0.2 mmol/kg gadolinum-DTPA (Berlex, Wayne, NJ). Appropriate coverage of the left atrium was obtained using 64 slices with a thickness of 2 mm and a matrix size of 108–156 × 192 (FOV 400, TR/TE 2.6/0.9, flip angle 15°). A timing bolus was performed to maximize enhancement of the left atrium.

Time Volume Curves

Using Argus software (Siemens Medical Solutions, Malvern, PA), the inner border of the left atrium was manually traced for each frame of each cine slice. The left atrial appendage and pulmonary veins were excluded at their junction with the left atrium on each image. The volume in each slice was calculated by multiplying the area of left atrium in the slice by the thickness

of the slice. The volumes measured in each slice were added together to determine the overall LAV (Simpson's Method of Disks). The volumes were plotted as a function of time to generate time volume curves. The maximum left atrial volume (LAMAX or α), the pre-atrial contraction volume (PACV or β), and the minimum left atrial volume (LAMIN) were measured. The global left atrial ejection fraction (LAEF) was calculated using the following formula: (LAMAX − LAMIN)/LAMAX. The LAEF was further divided into conduit (CEF) and pump (PEF) portions (Figure 1).

LA Volume Measurements

Commonly used echocardiographic measures of LAV were simulated using the area-length (AL) and ellipsoid (EL) models from 2-chamber and 4-chamber SSFP cines obtained during the CMR study(14). Aquarius software (Tera Recon, San Mateo, CA) was used to measure the LAV on the MRA.

Regional LA Displacement

The maximum in-plane displacement of the posterior aspect of each of the major pulmonary veins (LUPV, LLPV, RUPV, RLPV) was measured from the axial cines. The structure of interest was marked in the LAMAX image, the cine was advanced to the LAMIN frame, and the distance the structure moved was measured linearly. The in-plane displacement of the anterior left atrium at the level of the sino-tubular junction (AntLA) was also measured using the appropriate axial cine. The 3-chamber SSFP cine was used to measure the displacement of the postero-lateral mitral valve annulus (MITRAL). The 2-chamber view was used to measure the displacement of the ridge separating the left superior pulmonary vein and the left atrial appendage (LAA) (Figure 2).

Statistical Analysis

Continuous variables are expressed as mean ± standard deviation. The relationship between the LAV (calculated by MRA, area-length model, or ellipsoid model) and the time-volume curve was determined using Bland-Altman plots and linear regression analysis. One-way ANOVA was used to measure differences in regional displacement. A p value <0.05 was considered significant. Analysis was performed using GraphPad Prism version 4.0c for Macintosh (GraphPad Software, San Diego, CA).

Results

Patient characteristics are listed in Table 1. The LAV changed substantially during the cardiac cycle (Figure 1), and the overall LAEF was 45±10% (range 15% to 61%). The LAMAX was 107±36ml and occurred at 42±5% (range 29% to 51%) of the RR interval. The LAMAX ranged from 51ml to 188ml. Following passive emptying, the volume fell to 81±34ml (range 34ml to 169ml). The conduit ejection fraction was 25±9% (range 10% to 40%). Passive emptying was followed by a brief period of diastasis that began at 65±7% (range 50% to 80%) of the RR interval and was followed by active contraction. The PACV was 86±34ml and occurred at 81 ±4% (range 71% to 90%) of the RR interval. The PACV ranged from 34ml to 170ml. The pump ejection fraction was 31±10% (range 6% to 48%). After LA contraction, the residual volume was 61±32ml and ranged from 21ml to 159ml. Linear regression analysis (Figure 3) revealed that as LAMAX increased, LAEF decreased with a slope of −0.20±0.03 (r^2=0.50, $p<0.0001$). LAMAX had a similar influence on the conduit ejection fraction (slope= −0.13 ±0.04, r^2=0.30, p=0.002) and the pump ejection fraction (slope= −0.16±0.04, r^2=0.35, p=0.0006). Additionally, the three slopes were not different from each other (p=0.416) suggesting that the LAMAX influenced all three measurements of left atrial function similarly. Figure 3 also shows that there is no significant relationship between LAMAX and the timing to LAMAX (r^2=0, p=0.97) and timing to PACV (r^2=0.02, p=0.43).

Static measurements of LAV measured using the MRA or commonly used echocardiographic methods such as the area-length model and ellipsoid model correlated well with both LAMAX (r^2= 0.57, 0.49, and 0.65, respectively, p<0.0001) and PACV (r^2= 0.62, 0.56, and 0.65, respectively, p<0.0001). Bland-Altman analysis (Figure 4) demonstrated that the LAMAX was underestimated by all 3 methods. The average measurement bias for MRA, area-length model, and ellipsoid model was −21±25ml, −16±26ml, and −35±22ml, respectively. The bias and limits of agreement were reduced when LAV measurements were compared to PACV rather than LAMAX.

Regional variation in left atrial displacement was determined (Figure 5). The posterior aspect of the pulmonary veins demonstrated minimal in-plane displacement (LLPV 2.7±1.2mm, LUPV 2.1±1.1mm, RLPV 1.9±1.1mm, and RUPV 2.3±1.0mm); whereas, the anterior left atrium, the postero-lateral mitral annulus, and the ridge of the left atrial appendage displaced significantly during the cardiac cycle (8.7±2.3mm, 12.5±3.9mm, and 9.8±3.4mm, respectively). The variation in displacement between regions was significant by ANOVA (p<0.0001).

Discussion

We have quantified the changes in LAV during the cardiac cycle in patients with paroxysmal AF while in sinus rhythm. LAMAX occurred immediately prior to mitral valve opening after which there was a period of passive emptying, a period of diastasis and finally atrial contraction. LAMIN was reached immediately prior to mitral valve closure. The time volume curves are illustrated in Figure 1. In addition, this study has shown that the posterior aspect of the pulmonary vein ostia are only minimally displaced; whereas, the postero-lateral aspect of the mitral annulus, the anterior aspect of left atrium, and the ridge between the LA appendage and left upper pulmonary vein demonstrate significant displacement. The magnitude and timing of these volume changes have important implications for the integration of CMR and CCT images with catheter geometries obtained during atrial fibrillation ablation procedures.

Methods of evaluating LA size

The left atrial size is often estimated using echocardiography, most simply with a single linear measurement of the antero-posterior diameter. However, unidimensional measures oversimplify the complex anatomy of the left atrium. Most investigators consider it to be more accurate to either directly measure LAV or estimate it using geometric models such as the area-length or ellipsoid models(15). The relationship of these measurements to the cardiac cycle is not well defined. Because the LAV is sensitive to changes in heart rate and preload and because echocardiography was not simultaneously performed, we simulated standard geometric models of LAV typically used during echocardiography using CMR. The present study demonstrates that both the area-length and ellipsoid models underestimate the maximum left atrial volume. A previous study suggested that LAV as measured by MRA correlated better with the pre-atrial contraction volume rather than with the maximal left atrial volume(16). Our study confirms this finding in patients with paroxysmal atrial fibrillation. In fact, the measured volume of all three techniques has a reduced bias and tighter limits of agreement when compared to the pre-atrial contraction volume rather than the maximal left atrial volume. The ungated MRA is a better measure of the PACV than the LAMAX likely because image acquisition occurs throughout the cardiac cycle, and the time volume curves reveal that the left atrial volume approximates the PACV for a significant portion of the cardiac cycle influencing the measured MRA volume. Similarly, both geometric models are also more representative of the PACV despite the fact that the measurements are made during maximal atrial size.

LA volume changes and AF ablation

Dynamic LAV changes have previously been studied using older CMR techniques in small cohorts of normal volunteers and children (17,18). We examined the changes in LAV over the entire cardiac cycle in patients with paroxysmal atrial fibrillation using a CMR technique with improved spatial and temporal resolution from the perspective of atrial fibrillation ablation. The concept of registering a static 3D CMR or CCT image to a catheter geometry of the LA at the time of the procedure and then using the 3D image for catheter navigation is attractive to physicians performing AF ablation. Such electroanatomical mapping systems have the potential to shorten procedure times, improve outcomes and reduce complications. Early versions of such software are now in clinical use but they are time consuming and not consistently accurate. Registration is performed in two ways: (1) By linking the 3D coordinates of the tip of the ablation catheter positioned at prominent landmarks (eg. the ostium of pulmonary veins) with the corresponding location on the 3D image or (2) creating a catheter geometry by sweeping the catheter across the surface of the LA to collect hundreds of points to generate a 3D image. The catheter geometry image is then linked with the surface of the 3D CMR image using a best fit algorithm. One or both of these methods may be used but the second, known as surface registration, appears to be more accurate.

In order to study the registration process and possible problems encountered during atrial fibrillation ablation, we selected cardiac MRI as a model to learn from. Benefits of selecting CMR as a model include the absence of ionizing radiation and an excellent temporal and spatial resolution. Although, we obtained our data using CMR, the challenges for image registration during an atrial fibrillation procedure would be the same for cardiac CT. The changes in LAV during the cardiac cycle demonstrated in our study are highly clinically relevant to the registration of 3D images and have significant implications for this registration process. In fact, our data suggest that there are large fluctuations in LAV during the cardiac cycle. On average, the LAMAX was 107ml; whereas, the minimum volume was only 61ml. In addition to the volume changes that occurred during the cardiac cycle, there was a significant variability among patients in the degree of volume change. The conduit ejection fraction ranged from 10% to 40% and the pumping ejection fraction ranged from 6% to 48%. Given a constant change in volume during the cardiac cycle, it appears that the best registration accuracy would be achieved by acquiring the CCT or CMR images and the catheter geometry at the same point in the cardiac cycle. Typically, CCT is gated to approximately 70 percent of the RR interval and CMR angiography is ungated, but there is no universal standard. Catheter geometry can be collected either using ECG gating or alternatively, by continuously collecting points through all phases of the cardiac cycle. The latter is quicker, gives a smoother looking geometry, and is thus generally preferred. Continuous collection of points is likely to introduce error in the volume of such a catheter geometry and likely represents maximum LA volume. This error will be compounded when the catheter geometry is registered to a static 3D image representing PACV. ECG gating may be inaccurate in patients who are in atrial fibrillation at the time of the study, and the effects of AF on LA volume change during the cardiac cycle remain unknown.

ECG gating needs to be considered when choosing between imaging modalities and specific protocols. Angiograms obtained using CMR are typically ungated. The resultant image set has blurred borders and the left atrial image is a volume average of the various left atrial positions that occur during the 15–20 second scan period. Furthermore, the spatial resolution often must be as low as 2mm in order to provide adequate image signal to be used with most of the current ablation software. Although CCT images are electrocardiographically gated, have excellent spatial resolution, and have an adequate contrast to noise ratio, the ideal portion of the cardiac cycle for use during ablation procedures has not been well defined. Additionally, the technique requires the use of iodinated contrast and has a significant radiation burden. It has previously

been shown that standard echocardiographic volume measurements of the left atrium underestimate the electroanatomical catheter geometry by 23%(19). In our study, we show that ungated MRA underestimates the maximum left atrial volume by 21%. The left atrium is clearly a dynamic structure that moves substantially, not only during the cardiac cycle, but also during respiration; furthermore, the LAV depends on preload and even patient position. Integration of CMR or CCT images with those acquired in the electrophysiology lab must take into account these changes.

LA regional wall motion and LA image integration

In addition to changes in LAV during the cardiac cycle, there are regional variations in left atrial motion that may impact the integration of CCT and CMR images with catheter geometry. The displacement data demonstrate that the appropriate selection of fiducial points for image integration is an important area of investigation. Our data reveal that very little motion occurs in the posterior aspect of the pulmonary veins; therefore, the pulmonary vein ostia should be incorporated into future schemes for the registration of left atrial images. It has previously been shown that the diameter of the pulmonary vein ostia changes over the cardiac cycle and that the pulmonary veins enter the LA at a variety of angles (13). It is possible that the significant LAV changes that occur during the cardiac cycle influence the angle at which the pulmonary veins are entering the LA at any given point. The volume changes may also lead to splaying of the pulmonary veins. The mitral annulus, the anterior aspect of left atrium, and the ridge between the LA appendage and LU pulmonary vein are mobile and, if used as fiducial points for registration, are likely to introduce error. The regional variation of left atrial motion should also be considered when ablation targets are chosen.

Other clinical implications

The size of the left atrium is an important determinant of prognosis(20–22) and predicts the likelihood of AF recurrence after restoration to normal sinus rhythm(23). It is unclear if LAMAX is a more important predictor of prognosis and response to therapy than traditional measures of left atrial size. Kaminski et al recently suggested that left atrial pump function is a better predictor of adverse cardiovascular events in hypertensive patients than left atrial size (24). Additionally, improvement in left atrial function has been noted after cardiac resynchronization for the treatment of heart failure(25). Atrial function is restored when the heart is returned to sinus rhythm, but whether atrial function post-ablation improves or declines compared to controls is controversial(26–28). The impact of scar formation, which has been shown to include around 30% of the LA endocardium, on contractility and conduction patterns is not fully understood(29). It is possible that the impact of scar in the posterior aspect of the left atrium is minimized due to its minimal contribution to left atrial motion, but there may be a reduction in left atrial function if fibrosis created during the ablation procedure extends into more mobile portions of the left atrium. Recently Peters et al used high resolution CMR to detect scar created by an ablation procedure(30). Although they detected the presence of new scar in all the patients, it circumferentially encompassed the pulmonary vein in only 62%. They also noted that the transmural extent of the affected tissue was inversely related to the time from procedure. It remains to be seen whether scar imaging can be used to predict which patients will have a recurrence of atrial fibrillation and which patients will have an improved left atrial function following a pulmonary vein isolation procedure.

Conclusions

We conclude that there are significant changes in LAV during the cardiac cycle in patients with a history of paroxysmal atrial fibrillation. In addition, most current measures of LAV significantly underestimate the maximum left atrial volume. The dynamic nature of the LAV and regional motion should be considered prior to atrial fibrillation ablation. The volume and

morphology of a static 3D image, either as a catheter geometry or as a CCT or CMR image, will be significantly affected by the timing of data acquisition. The same standard for data acquisition should be used for creation of each of these 3D models to facilitate accurate image registration during electroanatomical mapping. A simple clinical solution might be to electrocardiographically gate the electro-anatomical maps and the CCT or CMR images at the same part of the cardiac cycle.

Acknowledgements

Amit Patel is supported by NIH Grant: 5-T32 EB003841

Glossary of Abbreviations

AF
atrial fibrillation

LA
left atrium

LAV
left atrial volume

CCT
cardiac computed tomography

CMR
cardiac magnetic resonance

MRA
magnetic resonance angiography

SSFP
steady state free precession

LAEF
left atrial ejection fraction

PEF
left atrial pump ejection fraction

CEF
left atrial conduit ejection fraction

LAMAX
maximum left atrial volume

LAMIN
minimum left atrial volume

PACV
pre-left atrial contraction volume

AL
area-length model

EL
ellipsoid model

PV
pulmonary vein

RUPV
right upper pulmonary vein

RLPV
right lower pulmonary vein

LUPV
left upper pulmonary vein

LLPV
left lower pulmonary vein

AntLA
anterior left atrium

LAA
left atrial appendage

LVEF
left ventricular ejection fraction

References

1. Haissaguerre M, Jais P, Shah DC, et al. Electrophysiological end point for catheter ablation of atrial fibrillation initiated from multiple pulmonary venous foci. Circulation 2000;101:1409–17. [PubMed: 10736285]
2. Pappone C, Rosanio S, Oreto G, et al. Circumferential radiofrequency ablation of pulmonary vein ostia: A new anatomic approach for curing atrial fibrillation. Circulation 2000;102:2619–28. [PubMed: 11085966]
3. Nademanee K, McKenzie J, Kosar E, et al. A new approach for catheter ablation of atrial fibrillation: mapping of the electrophysiologic substrate. J Am Coll Cardiol 2004;43:2044–53. [PubMed: 15172410]
4. Kanagaratnam L, Tomassoni G, Schweikert R, et al. Empirical pulmonary vein isolation in patients with chronic atrial fibrillation using a three-dimensional nonfluoroscopic mapping system: long-term follow-up. Pacing Clin Electrophysiol 2001;24:1774–9. [PubMed: 11817811]
5. Weiss C, Willems S, Risius T, et al. Functional disconnection of arrhythmogenic pulmonary veins in patients with paroxysmal atrial fibrillation guided by combined electroanatomical (CARTO) and conventional mapping. J Interv Card Electrophysiol 2002;6:267–75. [PubMed: 12154329]
6. Tse HF, Lee KL, Fan K, et al. Nonfluoroscopic magnetic electroanatomic mapping to facilitate focal pulmonary veins ablation for paroxysmal atrial fibrillation. Pacing Clin Electrophysiol 2002;25:57–61. [PubMed: 11877938]
7. Novak PG, Guerra PG, Thibault B, et al. Utility of a nonfluoroscopic navigation system for pulmonary vein isolation. J Cardiovasc Electrophysiol 2004;15:967. [PubMed: 15333100]
8. Verma A, Marrouche N, Natale A. Novel method to integrate three-dimensional computed tomographic images of the left atrium with real-time electroanatomic mapping. J Cardiovasc Electrophysiol 2004;15:968. [PubMed: 15333101]
9. Reddy VY, Malchano ZJ, Holmvang G, et al. Integration of cardiac magnetic resonance imaging with three-dimensional electroanatomic mapping to guide left ventricular catheter manipulation: feasibility in a porcine model of healed myocardial infarction. J Am Coll Cardiol 2004;44:2202–13. [PubMed: 15582319]
10. Dong J, Calkins H, Solomon SB, et al. Integrated electroanatomic mapping with three-dimensional computed tomographic images for real-time guided ablations. Circulation 2006;113:186–94. [PubMed: 16401772]

11. Kistler PM, Earley MJ, Harris S, et al. Validation of three-dimensional cardiac image integration: use of integrated CT image into electroanatomic mapping system to perform catheter ablation of atrial fibrillation. J Cardiovasc Electrophysiol 2006;17:341–8. [PubMed: 16643352]
12. Ho SY, Sanchez-Quintana D, Cabrera JA, et al. Anatomy of the left atrium: implications for radiofrequency ablation of atrial fibrillation. J Cardiovasc Electrophysiol 1999;10:1525–33. [PubMed: 10571372]
13. Mansour M, Holmvang G, Sosnovik D, et al. Assessment of Pulmonary Vein Anatomic Variability by Magnetic Resonance Imaging: Implications for Catheter Ablation Techniques for Atrial Fibrillation. Journal of Cardiovascular Electrophysiology 2004;15:387–93. [PubMed: 15089984]
14. Lang RM, Bierig M, Devereux RB, et al. Recommendations for chamber quantification: a report from the American Society of Echocardiography's Guidelines and Standards Committee and the Chamber Quantification Writing Group, developed in conjunction with the European Association of Echocardiography, a branch of the European Society of Cardiology. J Am Soc Echocardiogr 2005;18:1440–63. [PubMed: 16376782]
15. Lester SJ, Ryan EW, Schiller NB, et al. Best method in clinical practice and in research studies to determine left atrial size. Am J Cardiol 1999;84:829–32. [PubMed: 10513783]
16. Hauser TH, McClennen S, Katsimaglis G, et al. Assessment of left atrial volume by contrast enhanced magnetic resonance angiography. J Cardiovasc Magn Reson 2004;6:491–7. [PubMed: 15137333]
17. Jarvinen V, Kupari M, Hekali P, et al. Assessment of left atrial volumes and phasic function using cine magnetic resonance imaging in normal subjects. Am J Cardiol 1994;73:1135–8. [PubMed: 8198044]
18. Poutanen T, Ikonen A, Vainio P, et al. Left atrial volume assessed by transthoracic three dimensional echocardiography and magnetic resonance imaging: dynamic changes during the heart cycle in children. Heart 2000;83:537–42. [PubMed: 10768903]
19. Patel VV, Ren JF, Jeffery ME, et al. Comparison of left atrial volume assessed by magnetic endocardial catheter mapping versus transthoracic echocardiography. Am J Cardiol 2003;91:351–4. [PubMed: 12565098]
20. Moller JE, Hillis GS, Oh JK, et al. Left Atrial Volume: A Powerful Predictor of Survival After Acute Myocardial Infarction. Circulation 2003;107:2207–12. [PubMed: 12695291]
21. Rossi A, Cicoira M, Zanolla L, et al. Determinants and prognostic value of left atrial volume in patients with dilated cardiomyopathy. J Am Coll Cardiol 2002;40:1425–30. [PubMed: 12392832]
22. Osranek M, Bursi F, Bailey KR, et al. Left atrial volume predicts cardiovascular events in patients originally diagnosed with lone atrial fibrillation: three-decade follow-up. Eur Heart J 2005;26:2556–61. [PubMed: 16141257]
23. Berruezo A, Tamborero D, Mont L, et al. Pre-procedural predictors of atrial fibrillation recurrence after circumferential pulmonary vein ablation. Eur Heart J 2007;28:836–41. [PubMed: 17395676]
24. Kaminski MA, Khin MM, Hauser TH, et al. Strong Prognostic Implication of Left Atrial Conduit and Pump Functions Assessed by Cardiac magnetic Resonance in Hypertensive Patients At Risk for Diastolic Dysfunction. AHA Scientific Sessions 2006:Abstract 3777.
25. Yu C-M, Fang F, Zhang Q, et al. Improvement of Atrial Function and Atrial Reverse Remodeling After Cardiac Resynchronization Therapy for Heart Failure. J Am Coll Cardiol 2007;50:778–85. [PubMed: 17707183]
26. Verma A, Kilicaslan F, Adams JR, et al. Extensive ablation during pulmonary vein antrum isolation has no adverse impact on left atrial function: an echocardiography and cine computed tomography analysis. J Cardiovasc Electrophysiol 2006;17:741–6. [PubMed: 16836670]
27. Callans DJ. The effect of catheter ablation for atrial fibrillation on left atrial transport function. [comment]. Journal of Cardiovascular Electrophysiology 2006;17(7):747–8. [PubMed: 16836671]
28. Lemola K, Desjardins B, Sneider M, et al. Effect of left atrial circumferential ablation for atrial fibrillation on left atrial transport function.[see comment]. Heart Rhythm 2005;2(9):923–8. [PubMed: 16171744]
29. Takahashi Y, O'Neill MD, Hocini M, et al. Effects of stepwise ablation of chronic atrial fibrillation on atrial electrical and mechanical properties. Journal of the American College of Cardiology 2007;49 (12):1306–14. [PubMed: 17394963]

30. Peters DC, Wylie JV, Hauser TH, et al. Detection of Pulmonary Vein and Left Atrial Scar after Catheter Ablation with Three-dimensional Navigator-gated Delayed Enhancement MR Imaging: Initial Experience. Radiology 2007;243:690–5. [PubMed: 17517928]

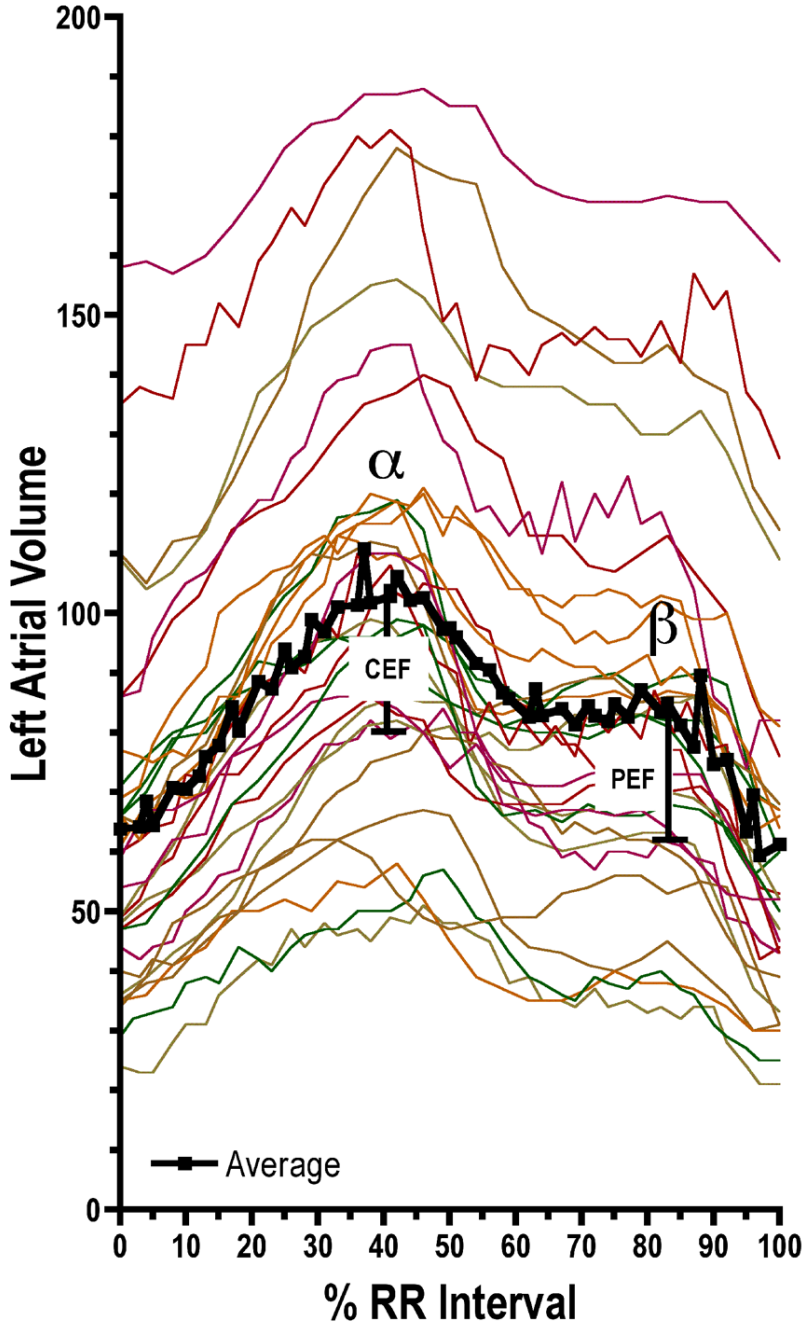

Figure 1.

Each line represents the unique time volume curve (TVC) for each of the 30 patients. The dark-bold line represents the "average" TVC. α represents LAMAX which is 107±36ml and ranged from 51ml to 188ml. β represents the PACV which is 86±34ml and ranged from 34ml to 170ml. Measurements for the conduit ejection fraction (CEF) and pump ejection fraction (PEF) are noted and were 25±9% and 31±10%, respectively. The reduction in LAV following α represents mitral valve opening. In addition to the variation in volume present in the cohort, a variety of 'patterns' in left atrial filling and emptying are present. These patterns are reflected by the different filling and emptying slopes and by the relative contribution of mitral valve opening and atrial systole.

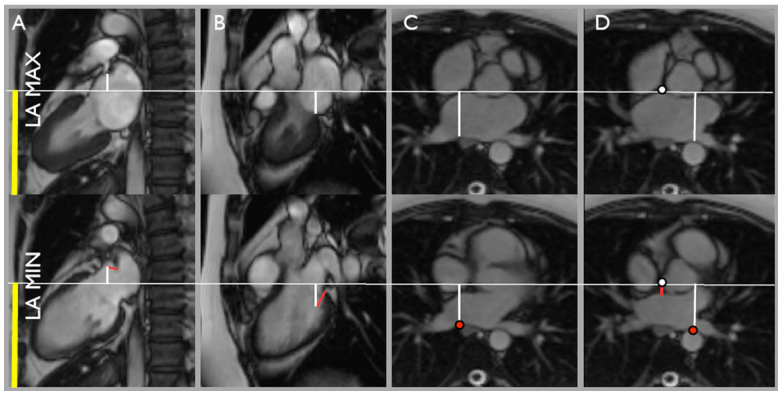

Figure 2.

Several views of the left atrium during its maximum and minimum volume are shown. A horizontal white line is drawn through the center of each image as a point of reference and the identically sized yellow vertical line on the left border of the image confirms that the horizontal reference line is equally positioned on the LAMAX and LAMIN images. The red lines on the LAMIN images represent the in-plane displacement of various points of interest. The red dots represent the lack of significant motion. The top row represents LAMAX and the bottom row represents LAMIN. Panels A, B, and D respectively show the ridge separating the left upper pulmonary vein and the left atrial appendage (LAA), the postero-lateral mitral valve annulus (MITRAL), and the anterior left atrium at the level of the sino-tubular junction which is represented by the white dot (AntLA). The posterior aspects of the right lower pulmonary vein (RLPV) and the left lower pulmonary vein (LLPV) are shown in panels C and D.

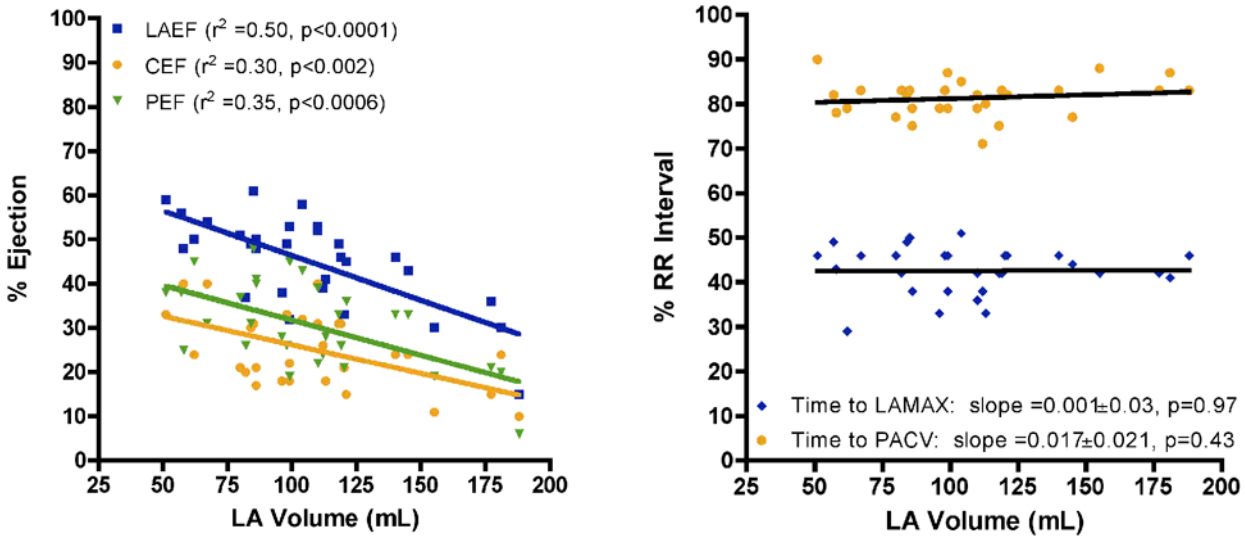

Figure 3.

On the left, linear regression analysis shows that global left atrial ejection fraction (LAEF) and its conduit (CEF) and pumping (PEF) components are inversely related to LAV (maximum volume). The graph on the right shows that no significant relationship exists between the LAV and the timing of the LA ejection cycle.

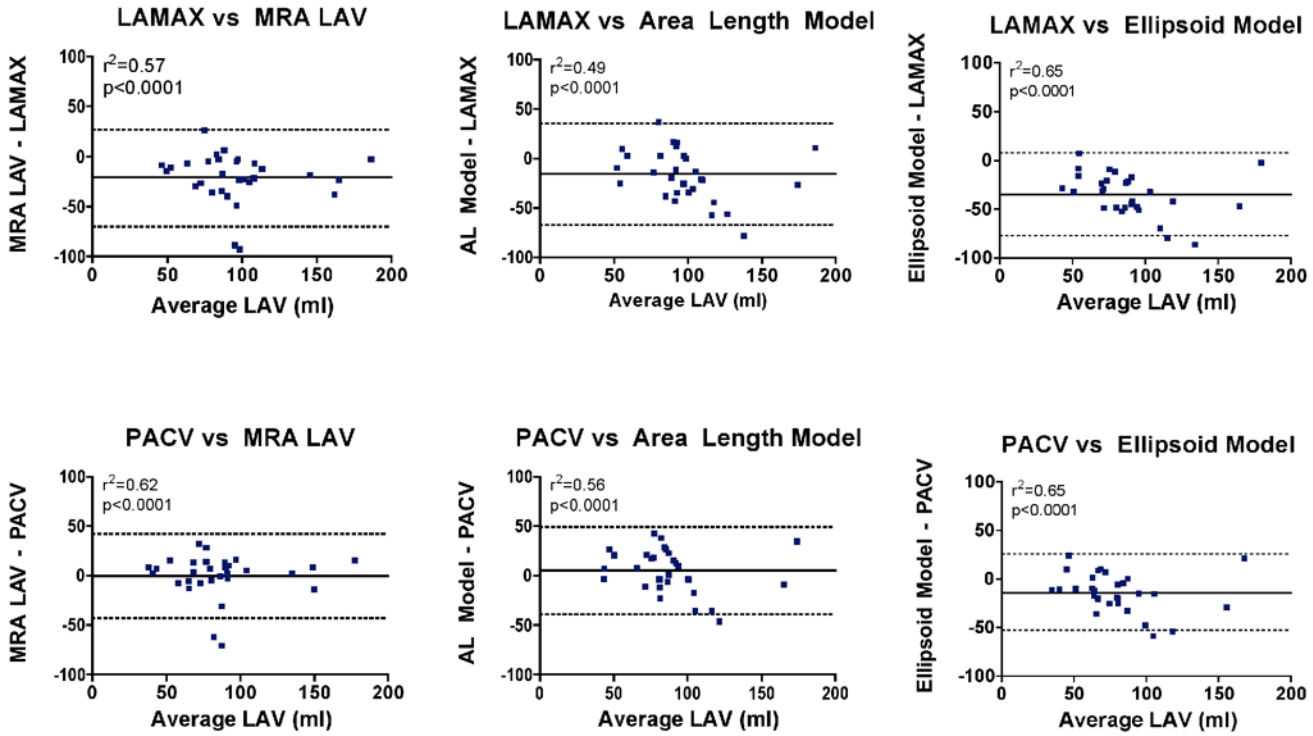

Figure 4.

Bland-Altman plots reveal the relationship of the left atrial volume (LAV) as measured from a magnetic resonance angiogram (MRA), the area-length model (AL), and the ellipsoid model (EL) with the maximum left atrial volume (LAMAX) and pre-atrial contraction volume (PACV) as determined by the gold-standard time volume curves. LAMAX is underestimated by MRA, AL, and EL. The bias and limits of agreement are reduced when MRA, AL, and EL are compared to PACV.

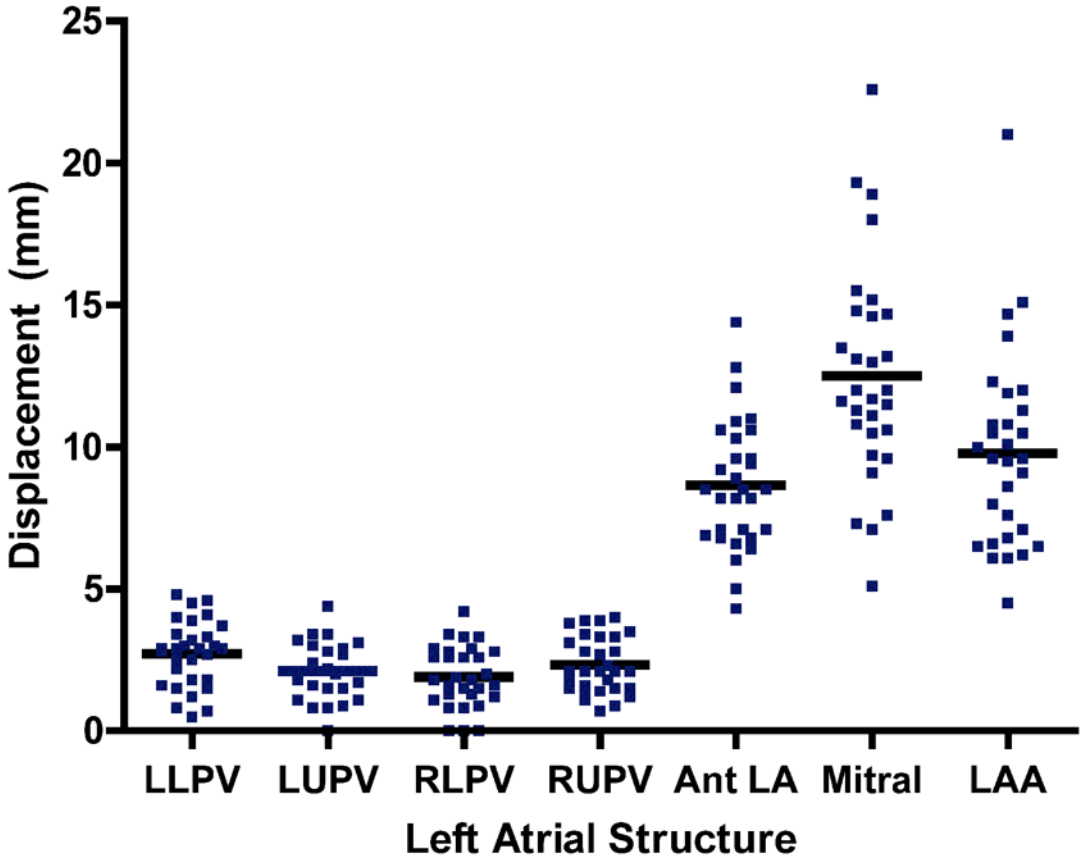

Figure 5.
The posterior aspects of the pulmonary vein ostia are minimally displaced; where as, the anterior left atrium at the level of the sino-tubular junction (AntLA), the postero-lateral mitral valve annulus (MITRAL), and the ridge separating the left superior pulmonary vein and the left atrial appendage (LAA) exhibit substantially more motion.

Table 1

Patient Characteristics (n = 30)

Age	56±12
Gender (male)	23 (77%)
Race (Caucasian)	30 (100%)
Height (inches)	70±4
Weight (kg)	94±20
BSA	29.5±5.4
Heart Rate	65±9 bpm
Past Medical History	
Hypertension	17 (57%)
Diabetes Mellitus	4 (13%)
Coronary Artery Disease	6 (20%)
Obese	14 (47%)
Other	
LVEF <50%	2 (7%)